Int J Adv Manuf Technol
DOI 10.1007/s00170-017-0703-5

ORIGINAL ARTICLE

Uncertainty quantification and management in additive manufacturing: current status, needs, and opportunities

Zhen Hu[1] · **Sankaran Mahadevan**[2]

Received: 9 March 2017 / Accepted: 19 June 2017

Abstract One of the major barriers that hinder the realization of significant potential of metal-based additive manufacturing (AM) techniques is the variation in the quality of the manufactured parts. Uncertainty quantification (UQ) and uncertainty management (UM) can resolve this challenge based on the modeling and simulation of the AM process. This paper reviews the research state of the art and discusses needs and opportunities in the UQ/UM of the AM processes, with a focus on laser powder bed fusion AM. The major methods and models of laser powder bed fusion AM process are summarized first. The current research work in UQ of AM processes is then reviewed. Based on the review of AM process models and current UQ approaches for the AM process, this paper presents insights into how the current state of the art UQ and UM techniques can be applied to AM to improve the product quality. Future research needs in UQ and UM of AM are also discussed. Laser sintering of metal nanoparticles, which is part of the micro-AM process, is used as an example to illustrate the application of UQ and UM in the AM.

Keywords Additive manufacturing · Uncertainty quantification · Uncertainty management · Metal · Powder bed

✉ Sankaran Mahadevan
sankaran.mahadevan@vanderbilt.edu

[1] Department of Civil and Environmental Engineering, Vanderbilt University, Nashville, TN 37235, USA

[2] Department of Civil and Environmental Engineering, Department of Mechanical Engineering, Vanderbilt University, Nashville, TN 37235, USA

1 Introduction

Additive manufacturing (AM) of metal components is a process of manufacturing metal components layer by layer based on 3D computer-aided design (CAD) models [1]. AM is opposite to traditional manufacturing, which usually subtracts materials through a series of processes like casting, molding, and machining [2]. Since it does not require special tools for part fabrication, it has high flexibility in manufacturing metal parts with any customized geometry. This characteristic gives AM significant potential in reducing material waste and manufacturing time. The manufacturing of metal components with highly complicated geometry is difficult to be accomplished using conventional manufacturing technologies. AM has been successfully demonstrated in the manufacturing of both metal components with complicated geometries (e.g., engine blade) and components at microsize level (i.e., microelectromechanical systems) [3]. Reports indicate that the market potential of AM techniques can reach several billion dollars [4].

Current AM techniques for metal component manufacturing include stereolithography (SLA) [5], fused deposition modeling (FDM) [6], laminated object manufacturing (LOM) [7], selective laser sintering (SLS) [8], selective laser melting (SLM) [9], direct metal deposition (DMD) [10], laser metal deposition (LMD) [11], direct metal laser melting (DMLM) [12], and others. One of the most widely used AM process for the manufacturing of metal components is powder bed fusion [13], where the powder is delivered to the powder bed layer by layer and melted by the laser beam according to specific laser paths every time a new layer of powder is added. From powder bed forming to melting and solidification, various sources of uncertainty are involved in the processes. These sources of uncertainty result in variability in the quality

Published online: 08 July 2017

of the manufactured component. The quality variation hinders consistent manufacturing of products with guaranteed high quality. This becomes a major hurdle for the wide application of AM techniques, especially in the manufacturing of metal components.

To achieve the quality control of the AM process, a good understanding of the uncertainty sources in each step of the AM process and their effects on product quality is needed. Uncertainty quantification (UQ) is a process of investigating the effects of uncertainty sources (aleatory and epistemic) on the quantities of interest (QoIs) [14–16]. Even though UQ for models of physical hardware has been intensively studied during the past decades and continue to address important research questions, UQ in AM is still at its early stage. Only a few examples have been reported in the literature [17–19]. In addition, currently reported UQ methods for AM are mainly based on experiments and are performed at the process level. This will result in excessive material wastage, increased product development cost, and delay in the product development process [20] because UQ usually requires numerous experiments and process optimization and UQ are implemented in a double loop framework (i.e., UQ needs to be performed repeatedly when the process is changed). A generic UQ framework built upon the understanding of fundamental principles of the AM will significantly benefit the wider acceptance of the AM process and push the AM techniques for the manufacturing of metal products to the next stage. Systematic UQ of AM will also provide a solid foundation for the uncertainty management (UM) of the AM process, thus allowing effective allocation of limited resources to meet quality requirement and robustness targets.

This paper aims to provide insights into UQ and consequently UM in the AM process, based on the review of currently AM process models and UQ approaches. The challenges related to the UQ of AM process are first discussed. Solutions of these challenges will then be presented through the employment of the state of the art UQ techniques. Future needs in UQ and UM of AM will be investigated as well. Finally, a laser sintering model of iron nanoparticles, an important step in the micro-AM, is used to illustrate the application of UQ techniques in AM of metal products. The contributions of this paper are summarized as follows: (1) a brief review of laser powder bed fusion-based AM process models; (2) a brief review of current state of the art of UQ in AM; (3) insights on UQ and UM of the AM process for manufacturing of metal products; (4) illustration of the application of state-of-the-art UQ techniques to the laser sintering of nanoparticles; and (5) identification of future needs for UQ/UM in AM.

The remainder of the paper is organized as follows. Section 2 provides a brief literature survey of the AM models for laser powder bed fusion-based manufacturing of metal products. Section 3 presents the state of the art in UQ and UM of AM processes. Section 4 discusses the insights and future needs for UQ and UM in AM. Laser sintering of nanoparticles is used to demonstrate some of the main UQ methods in Sect. 5, and concluding remarks are given in Sect. 6.

2 Literature survey of AM models

Figure 1 shows an illustration of the laser powder bed fusion system. Even if the actual AM system may be different for different manufacturing applications, the systems can be simplified similar to Fig. 1.

During the manufacturing process, the 3D model of a to-be-manufactured product is created first in a computer-aided design (CAD) software [21]. The 3D model is then converted into an STL file, which is sliced into layers according to the building orientation and slice thickness. This information is then converted into digital data for laser path planning. To form the metal powder bed for laser sintering, the powder delivery system will deliver a layer of powder to the fabrication system using the delivery piston and powder recoater mechanism. The powder is then melted by the laser following the laser paths. The fabrication system will decline to a certain level once the sintering of current layer is finished, and a new layer of powder is added for melting. This process is repeated until the manufacturing is finished. During this process, the scanner system and temperature sensor are used to monitor the process and a control system is used to coordinate the movements of the manufacturing system components.

There are several controllable process parameters in the AM process, such as laser scan speed, laser power, laser beam diameter, laser type, material type, radius of the powder, hatch spacing, building orientation, slice thickness, powder bed temperature, and others. Changing these parameters will not only affect the quality of the manufactured product but also influence the energy and material used during the manufacturing process. In order to determine the optimal process parameters, a good understanding of the AM process is required. During the past decade, AM process models have been developed mainly from the following six perspectives.

Energy consumption model The energy consumption model quantifies the total energy used to manufacture a component [22]. The total energy is roughly divided into five parts [22, 23], namely energy used by the laser system, energy used in moving the part and pistons of the delivery and fabrication systems, energy used in forming the powder bed, energy spent in heating the powder bed, and other miscellaneous energy consumption. The energy consumption model was first expressed as a function of laser system parameters [24] and then extended by Paul and Anand [23] to connect energy consumption with process parameters

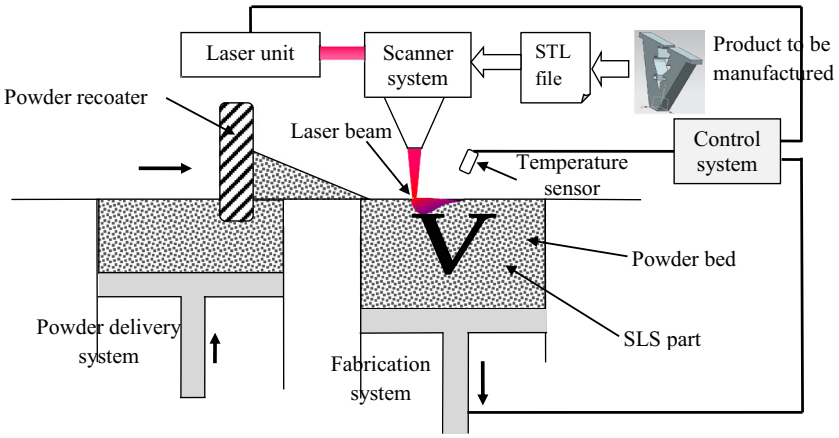

Fig. 1 Illustration of laser powder bed fusion

and part geometry. For instance, the laser energy consumption is modeled as [23]

$$E_L = (2\alpha P/(\pi dv))\text{TAS} \quad (1)$$

where E_L is the energy used by the laser system, α is the absorptive coefficient of the powder, P is the laser power, d is the laser beam radius measured on the powder bed, v is the laser scan speed, and TAS is the total area of sintering (TAS). The energy model is connected to the process parameters and component geometry through the TAS, which depends on the part geometry, slice thickness, and building orientation [23].

The energy consumption model has been applied to optimize the process parameters such as slice thickness and building orientation by minimizing the energy consumption. These energy models, however, are developed based on several assumptions and simplifications. For example, the absorptive coefficient is a parameter which is not straightforward to measure or estimate. This causes uncertainty in the output of the prediction model.

Heat source model The heat source model plays a vital role in understanding the effects of the heat source on the quality of the manufactured component. The horizontal intensity of the laser beam is usually modeled as a Gaussian distribution [25]. The vertical absorption distribution is more difficult to model since it is related to many factors such as material, distribution of particle size, laser beam size, and particle shape. Both direct measurements and simulation based methods have been explored for the estimation of powder absorptivity. For example, Rubenchik et al. [26] proposed a simple calorimetric scheme for the direct measurement of absorptivity of the powder bed. A detailed review of the direct measurement of powder absorptivity is available in Ref. [27]. The commonly used simulation method is the ray tracing method to evaluate the powder absorption. This method is similar to Monte Carlo simulation (MCS) and tracks the trajectories of single photons [28]. From the heat source modeling, it is found that the powder configuration and size distribution will affect the absorptivity of the powder bed significantly [29, 30].

Powder bed model The powder bed model provides information about the powder packing, such as packing density, particle size distribution, radial distribution, and porosity of the powder bed. It has been investigated using a raindrop model [31] and discrete element method (DEM) [32]; the latter is widely used at present. An open-source software LIGGGHTS is available to perform DEM for powder bed forming when the van der Waals forces can be overlooked [33, 34]. For example, Xin et al. [34] investigated the effects of a contact force and size distribution on the packing of microsized particles. Xiang et al. simulated the powder bed forming process using a nonlinear Hertzian contact model [35]. Herbold et al. [36] at Lawrence Livermore National Laboratory (LLNL) also developed a software for the simulation of powder layer deposition in AM using the DEM method. In these methods, it is typically assumed that the metal particles are spherical. In reality, however, the particles are often not perfect spheres [37].

Another challenge in powder bed modeling is the evolution of powder size distribution over time when the powders are recycled. The laser sintering will affect the powder size distribution if the powders are recycled. The information obtained from the powder bed model will be used in the heat source model and the melting pool model.

Melting pool model The melting pool model is one of the crucial models to investigate the effects of AM process on the microstructure and mechanical properties of the AM products. It is a multi-physics model related to thermodynamics and hydrodynamics. The currently available melting pool modeling approaches include lattice Boltzmann (LB) [38], a combined finite element (FE) and finite volume (FV) [39], a thermal model based on assumptions and simplifications [40], and a computational fluid dynamics (CFD) model by including heat transfer, melting, and Marangoni force [41]. The flow characteristics in the melting pool, surface tension, heat required for melting, influence of gravity, and the Marangoni convection all need to be accounted for in the melting pool model. The LB approach for melting pool model has been investigated using both 2D and 3D numerical methods [42].

When the 3D numerical method is used, the computational effort will be increased significantly. Software and toolboxes have also been developed for the melting pool model such as the routines in OpenFOAM [43] and ALE3D [44]. When AM is applied to the manufacturing of microsized components, the melting pool model needs to be modeled at the nanometer length scale. In that situation, a molecular dynamic simulation model can be employed for the simulation of melting [45].

From the melting pool simulation model, we can predict the porosity, surface roughness, melting pool shape, and thermal boundary conditions. The information obtained from the melting pool model will be used in the solidification and residual stress models to investigate the mechanical properties of the manufactured component.

Solidification model The solidification model investigates the microstructure evolution of the melting pool due to cooling after the laser sintering process, and is important for the prediction of the thermo-mechanical properties of the manufactured material. The grain size and grain morphology are simulated using the information of the temperature field obtained from the melting pool model. The widely used methods for the simulation of solidification are the phase field (PF) approaches, such as coupling of the LB approach with the cellular automaton (CA) models [46], and coupling of thermal FE and CA models [47, 48]. The metallurgical properties obtained from the solidification model will be used in the residual stress model. For example, the grain size which depends on the cooling rate will affect the hardness and tensile strength of the product. The information on tensile strength can be used for failure analysis in the macro-scale model. Experiment-based methods have also been investigated to study the solidification of metal fluid and validate the simulation models [49].

Residual stress model The residual stress model is used to evaluate the residual stress and product deformation due to heating and cooling during the manufacturing [50]. This model is usually developed at the macro-length scale. For micro-AM problems, it is at the microlength scale. Even though a mathematical model has been developed for the residual stress model based on simplifications and assumptions [51], the commonly used method is the thermo-mechanical FE analysis [52, 53]. The heat transfer analysis provides transient temperature field data, which is input to the mechanical analysis [54]. The residual stress model is connected with several QoIs such as manufacturing errors [55], fatigue life of the manufactured product, and failure strength of the product.

The above is a brief survey of AM models. More detailed reviews of two of the above reviewed models (i.e., melting pool model and solidification model) can be found in Refs. [27, 28, 54]. In Table 1, we summarize the models in the AM process in the context of the methods used to study the model and some of the main inputs and outputs of the models. This information will be used in Sect. 4 for the discussion of UQ and UM methods in AM.

The above review shows that all the AM models are connected with each other through various inputs and outputs. The integration of all the models will make the optimization of process parameters using computer simulation possible. Model-based AM process optimization through the integration of the simulation models is a promising research direction in future. Figure 2 illustrates the connections between different models and the relationships between process parameters and the QoIs. The length scales of different models are also provided in Fig. 2 for both normal AM and micro-AM.

3 UQ and UM in AM: state of the art

As discussed in Sect. 1, the variation in the quality of components produced from AM is a major barrier that impedes the realization of the full potential of AM techniques. To address this issue, UQ and UM have gained increasing attention in recent years. Current research efforts in UQ and UM of AM processes can be roughly classified into three groups: (1) UQ of AM using experiments, (2) UQ of melting pool model, and (3) UQ of solidification (microstructure) model. Detailed reviews of the three groups of efforts are given as follows.

Experiment-based UQ of AM process Most currently reported UQ research efforts in AM use physical experiments. This is due to the fact that advanced modeling and simulation techniques for AM process have been developed only in recent years. For UQ at the process level, AM experiments are performed repeatedly at different process parameter settings. Based on the data of QoIs collected at different input settings from physical experiments, the effects of process parameters on the quality of manufactured products are analyzed using statistical analysis [17, 79]. For instance, Delgado et al. [80] used analysis of variance (ANOVA) to evaluate the effects of scan speed, layer thickness and building orientation on dimensional error and surface roughness. Raghunath and Pandey [81] investigated the influence of process variables such as laser power, beam speed, hatch spacing, and scan length on the shrinkage of the product using signal-to-noise (S/N) ratio and ANOVA methods. By identifying the factors that have the most significant effects on the variation of product quality, the quality of AM can be improved by implementing quality control on the influential factors. Since physical experiments are usually expensive, research efforts on UQ of AM process have focused on effective design of experiments (DoE) [13]. Different sampling strategies, such as random sampling, stratified sampling, and Poisson disk sampling, have been investigated to improve the quality of samples in the design space [17]. The Taguchi method has also been employed to design experiments for the uncertainty analysis of AM [81, 82]. In

Table 1 Commonly available models in AM

Model	Methods	Inputs	Outputs
Energy [23, 55–60]	Connect energy consumption with total area of sintering (TAS) [23, 55, 59, 60], which is a function of slice thickness and building orientation	· Laser power · Beam diameter · Scan speed · Absorptivity of powder · Slice thickness · Building direction · Bed temperature	· Energy of laser system · Energy of moving powder and other systems · Energy of bed heating · Miscellaneous energy
Heat source [25, 26, 30, 61–66]	· Gaussian distribution for horizontal intensity · Direct measurement [26, 67] · Trajectory tracking of photons · Monte Carlo simulation (MCS)	· Material type · Powder distribution · Beam diameter · Laser power · Powder shape · Thermal diffusivity · Scan speed	· Absorbed energy · Absorption coefficients of materials · Vertical absorption distribution
Powder bed [34–36, 68, 69]	· Raindrop model · Discrete element method (DEM) · Nonlinear Hertzian contact model	· Sliding friction coefficient · Rolling friction coefficient · Young's modulus · Radius distribution · Hamaker constant · Damping coefficient · Restitution coefficient	· Packing density · Radial distribution function (RDF) · Porosity of the powder bed
Melting pool [18, 27, 40, 42, 54, 61, 70–74]	· Thermal model for melting · Lattice Boltzmann (LB) approach (2D and 3D) · Extended LB approach · Computational fluid dynamics (CFD) by including heat transfer, melting, and Marangoni force · OpenFOAM	· Scan speed · Laser power · Particle radial distribution · Absorption coefficient · Melting temperature · Thermal diffusivity · Layer thickness · Beam diameter	· Melt pool width · Melt pool shape · Diffusion efficiency · Cross-sectional area · Length-to-depth ratio · Porosity and layer bonding defects · Thermal boundary conditions · Surface roughness
Solidification [28, 47, 75, 76]	· Microscopic cellular automaton (CA) coupled with Macroscopic finite element (FE) approach · Phase field (PF) approach	· Cooling rate · Thermal history · Material properties	· Grain size · Thermo-mechanical properties of materials · Metallurgical properties
Residual stress [54, 77, 78]	· Couple finite volume (FV) with FE approach · Thermal-mechanical FE models	· Thermal boundary condition · Mechanical boundary condition · Material properties	· Residual stress · Shrinkage · Deformation · Fatigue life

order to build models for the experimental response, methods of Gaussian process modeling and other response surface models have been applied [17]. Correlation-based feature selection method has also been investigated to process the data obtained from physical experiments [27].

Even if the UQ of AM process based on physical experiments can achieve quality control to some extent, it has several disadvantages. For instance, it does not take advantage of currently available advanced simulation models of the AM process; this will result in a lot of material waste and delay in the product development process since experiments need to be performed repeatedly. The results cannot be applied to new components and designs because the effects of process parameters may change with problems. It is difficult to design an AM process to be robust to the variations in the environment using an experiment-based UQ approach. Effective analysis methods need to be developed for UQ based on a better understanding of the AM process using simulation models. In the context of model-based UQ, research efforts have been reported with respect to melting pool and solidification models.

UQ of melting pool As one of the most important models in the AM process, UQ of melting pool is of great interest to the researchers. For example, Schaaf performed uncertainty and sensitivity analysis for the melting pool model to identify the most sensitive parameters in the model [83]. Anderson proposed to use DAKOTA [84] and ALE3D software to explore UQ of the melting process [85]. Most recently, Lopez et al. [18] performed UQ for the metal melting pool model based on a thermal model developed by Devesse et al. [40]. They identified four sources of uncertainty in the melting pool model, namely model assumptions, unknown simulation parameters, numerical approximations, and measurement error [86]. In order to reduce the uncertainty, they incorporated the online measurement data into the model. Based on these efforts, the effects of uncertain parameters on the shape of the melting pool are studied.

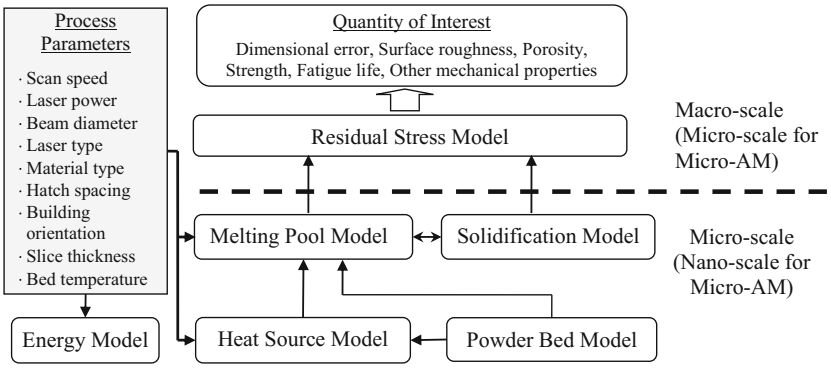

Fig. 2 Connections between different simulation models in the AM process

UQ of solidification Along with the research efforts in UQ of the melting pool model, efforts have also been devoted to UQ of the solidification model in recent years. Ma et al. [87] used design of experiments and FE models to identify the critical variables in laser powder bed fusion. Loughnane [88] has developed a UQ framework for microstructure characterization in AM. This framework accounts for sources of characterization errors, which are modeled using phantoms. Based on the modeling of error sources, effects of the errors on the microstructure statistics are analyzed. Statistical analysis and virtual modeling tools are also developed for the analysis of the microstructure. Park et al. [89] used a homogenization method to investigate the effect of microstructure on the mechanical properties in the macro-model. Cai and Mahadevan [90] studied the effect of cooling rate on the microstructure and considered various sources of uncertainty during the process of solidification.

The above literature review indicates that UQ and UM of AM process are still at its early stages. Figure 3 summarizes the three main UQ research efforts in the AM process and the associated methods.

A clear roadmap is needed for the development of UQ and UM methods in AM in order to realize the significant potential of AM of metal components. Inspired by this motivation, we provide insights and future needs on this research topic in the next section.

4 UQ and UM in AM: insights and future needs

In this section, we fist discuss the modeling of various sources of uncertainty in the AM process. Following that, UQ methods will be investigated. Based on the uncertainty modeling and UQ, we discuss future needs for UM in AM.

4.1 Modeling of uncertainty sources

We first identify the uncertainty sources in the AM and then discuss the modeling of these uncertainty sources.

4.1.1 Uncertainty sources analysis

Similar to many other UQ problems, the uncertainty sources in the AM process can be classified into two categories: *aleatory uncertainty* and *epistemic uncertainty* [91]. Aleatory uncertainty refers to natural variability, such as variability in the radius of the powder and fluctuation of laser scan speed, which is irreducible. Epistemic uncertainty refers to the uncertainty caused due to lack of knowledge, for example, difference between simulations and experiments and the numerical discretization errors in the lattice Boltzmann simulation. Epistemic uncertainty can be reduced by collecting more information. Both aleatory and epistemic uncertainty sources are involved in the AM process models (energy model, heat sources model, powder bed model, melting pool model, solidification model, and residual stress model) as reviewed in Sect. 2. These two categories of uncertainty sources in AM process are briefly summarized as follows.

Aleatory uncertainty Aleatory uncertainty sources are inherent in the AM process. It comes from the natural variability of parameters and variables. There are numerous sources of aleatory uncertainty. We only list several examples here. Some of the aleatory uncertainty sources include the variation of powder particle radius, the fluctuation of laser scan speed, diffusion coefficient of the material, friction coefficient, uncertainty of absorption coefficient, variation in the temperature boundary condition, and measurement errors. In Sect. 4.1.2,

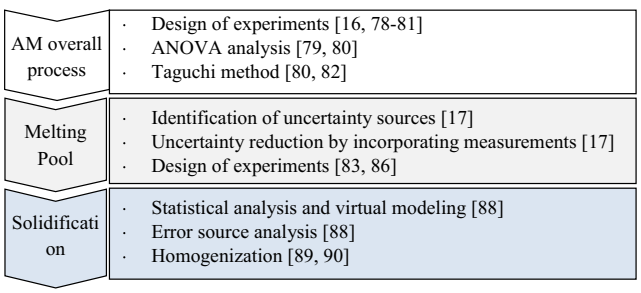

Fig. 3 Summary of three groups of existing UQ research in AM

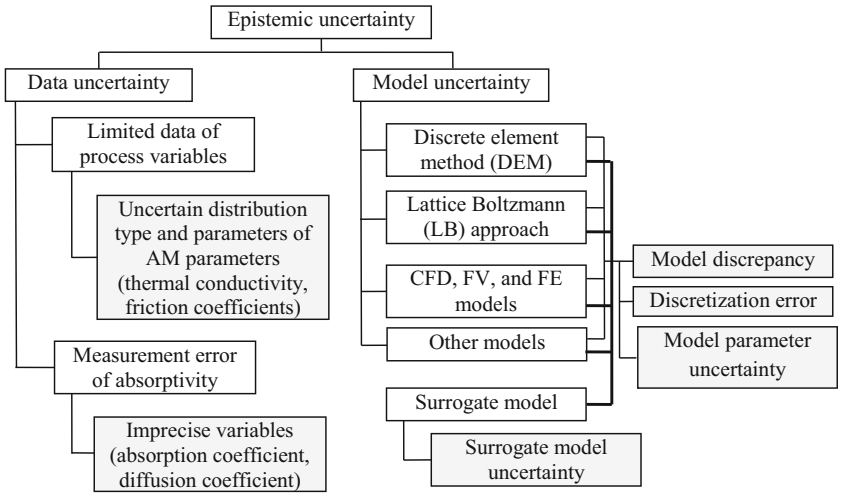

Fig. 4 Types of epistemic uncertainty sources in AM process

we will discuss how to model these sources of aleatory uncertainty.

Epistemic uncertainty As shown in Fig. 4, epistemic uncertainty can be further divided into two groups, namely *data uncertainty* and *model uncertainty* [92]. Data uncertainty may come from limited measurement data or imprecise measurements. For example, when the friction coefficients are modeled as random variables to represent the natural variability (aleatory uncertainty), there will be epistemic uncertainty in the distribution type and distribution parameters of the random variables if the amount of data is sparse. This case is quite common since in reality it is quite often the amount of data available is limited by resources. Even if some quantity is deterministic, we may not be able to precisely measure its value due to measurement error. In that situation, there is also epistemic uncertainty in the modeling of the AM process parameter, such as the absorptive coefficient of the material.

Along with the data uncertainty, the other important source of epistemic uncertainty is model uncertainty. Model uncertainty is used to model the difference between the computer simulation model and the experiment. Its quantification plays a role in correcting the simulation model to improve the accuracy of the simulation. The model uncertainty can be further classified into three groups, namely *model form uncertainty*, *solution approximation* (*including surrogate model uncertainty*), and *model parameter uncertainty*.

Model form uncertainty

- Model form uncertainty comes from the assumptions and simplifications made in the simulation models, for instance, the simplification made in the lattice Boltzmann approach for the modeling of melting pool and the assumptions made in the discrete element method for the simulation of powder bed model.

Solution approximation

- It comes from the numerical discretizations, reduced order modeling, or approximated solution methods in the simulation models. For example, the finite element or finite different simulations models solve the partial differential equations using numerical discretization. The computer simulation models are usually computationally expensive. Surrogate models are widely used to substitute the expensive simulation models. When the surrogate models are used, another source of model uncertainty called surrogate model uncertainty will be introduced. Since surrogate model is an approximation of the original model, it also belongs to the solution approximation.

Model parameter uncertainty

- In some simulation models, we are not able to exactly determine the values of some parameters. For example, we may not know the absorption coefficients of materials precisely. In this situation, we have uncertainty about the simulation models due to the uncertainty in the model parameters.

Next, we will discuss how to model various sources of uncertainty.

4.1.2 Modeling of uncertainty sources

(a) Modeling of aleatory uncertainty

A natural way of modeling the aleatory uncertainty is to use random variables for time-independent quantities and stochastic processes for time-varying quantities based on the classical frequency statistical theories [91]. When there is spatial variability, such as the spatially varying material properties in the melting pool model, the random field approach can be used to model the aleatory uncertainty. The combination of stochastic

process and random field methods can be applied to the modeling of aleatory uncertainty with both spatial and temporal variability [93].

(b) Modeling of data uncertainty

When the data for the modeling of aleatory uncertainty is too limited, the epistemic uncertainty in the parameters of the random variables, stochastic processes, random fields, or time-dependent random fields is modeled using the Bayes' theorem as [94]

$$f(\theta|\mathbf{D}) = P(\mathbf{D}|\theta)f(\theta)/\left(\int_\theta P(\mathbf{D}|\theta)f(\theta)d\theta\right) \propto P(\mathbf{D}|\theta)f(\theta) \quad (2)$$

where $\mathbf{D}$ is the observation data, θ is the vector of parameters of random variables, $P(\mathbf{D}|\theta)$ is the likelihood of observing the data $\mathbf{D}$, $f(\theta)$ is the prior distributions, $f(\theta|\mathbf{D})$ is the posterior distributions, and "∝" stands for "proportional to."

When there is uncertainty in both distribution type and distribution parameters, the posterior distributions of the ith distribution and its associated parameters can also be obtained using the Bayes' theorem as [95]

$$f(\theta_i,\ M_i|\mathbf{D}) = \frac{P(\mathbf{D}|\theta_i,\ M_i)f(\theta_i|M_i)P(M_i)}{\sum_{j=1}^{m} P(M_j)\int_\theta P(\mathbf{D}|\theta_j,\ M_j)f(\theta_j|M_j)d\theta_j} \propto P(\mathbf{D}|\theta_i,\ M_i)f(\theta_i|M_i)P(M_i) \quad (3)$$

where M_i is the ith distribution type, θ_i is the vector of parameters of the ith distribution type, $f(\theta_i|M_i)$ is the probability that the parameters of the ith distribution type is θ_i, and m is the total number of distribution types.

The data uncertainty in the aleatory variables can also be modeled using evidence theory [96], likelihood-based method [97], and interval variables [98] depending on the degree of uncertainty in the collected data. For example, we may only know that the absorption coefficient of a material is within a certain range. In that case, we can describe the uncertainty in the absorption coefficient as an interval variable.

The aforementioned methods focus on how to deal with aleatory uncertainty and epistemic uncertainty due to data uncertainty. The modeling of model uncertainty is more complicated than that of data uncertainty. In the subsequent section, we introduce the modeling of various sources of model uncertainty.

4.1.3 Modeling of model uncertainty

(a) Model solution approximation

Model discretization error is one source of model uncertainty due to solution approximation. It comes from the numerical discretizations in the simulation model. One of the commonly adopted methods for the modeling of discretization error is the Richardson extrapolation method [99, 100]. For a given input setting $\mathbf{d}$, the discretization error of the simulation results $y_s(\mathbf{d})$, of an Finite element analysis (FEA) simulation with mesh size h_1 can be quantified based on two more FEA simulations with finer mesh size h_2 and finest mesh size h_3 as follows [99, 100]

$$\varepsilon_{FEA}(\mathbf{d}) = \left[y_s^{(1)}(\ \mathbf{d}) - y_s^{(2)}(\ \mathbf{d})\right] \Big/ \left(r_{mesh}^{p_c} - 1\right), \quad (4)$$

where $y_s^{(k)}(\ \mathbf{d})$ is the result of FEA simulation with inputs $\mathbf{d}$ and mesh size h_k, $r_{mesh} = h_2/h_1 = h_3/h_2$ is the mesh refinement ratio, and the convergence p_c is estimated as $p_c = \ln\left[\left(y_s^{(3)}(\mathbf{d}) - y_s^{(2)}(\mathbf{d})\right) / \left(y_s^{(2)}(\ \mathbf{d}) - y_s^{(1)}(\mathbf{d})\right)\right] / \ln r_{mesh}$.

There are also other sources of uncertainty due to solution approximations, for example, the uncertainty due to reduced order modeling and uncertainty due to the use of surrogate models in the analysis. Since the melting pool model and the solidification model are computationally very expensive, surrogate models are often needed to substitute these simulation models. Due to the limited number of training points, we will have surrogate model uncertainty at untrained input settings when the surrogate model is used to perform predictions. Modeling of the surrogate model uncertainty will be discussed in detail in the following section.

(b) Model discrepancy and model parameter uncertainty

Model discrepancy or model form uncertainty comes from the assumptions and simplifications made in various simulation models. For example, the assumption of sphere particles of the powder in the DEM simulation, the simplification of melting pool models by ignoring the heat radiation and evaporation, and the simplification of Marangoni forces in the FV and FE combined melting pool model. If there is only model discrepancy or model form uncertainty, the model discrepancy can be modeled as a surrogate model by comparing the difference between the simulation model and the experiment at different input settings.

However, it is quite often that the model parameter uncertainty and model discrepancy are presented simultaneously in the simulation model. Since the some parameters are unknown due to the model parameter uncertainty and the model form uncertainty is a function of these model parameters, it is

very difficult to accurately model these two sources of model uncertainty together. A widely used approach for dealing with this kind of problem is the employment of *model calibration* approach under the Kennedy and O'Hagan framework (KOH framework) [101]. In the KOH framework, the model discrepancy term is modeled as a Gaussian process model. The hyper parameters of the Gaussian process model are then estimated based on the maximum likelihood estimation (MLE) approach using the prior information of the unknown model parameters. After the model discrepancy is approximated using a Gaussian process model, the unknown model parameters are estimated using the Bayesian calibration method based on the surrogate model of model discrepancy term. More details of the KOH framework are available in Ref. [101].

4.2 Uncertainty quantification

The purpose of UQ is to investigate the effects of uncertainty sources on the variation of the QoIs. Based on the modeling of uncertainty sources described in the last subsection, we investigate the UQ of AM process from two main perspectives, namely UQ of a single model and uncertainty aggregation across multiple models.

4.2.1 UQ of a single model

UQ of a single model can be performed for each individual model as summarized in Sect. 2. There are two types of UQ activities in the UQ of a single model: *local UQ and global UQ*. In local UQ, we are usually interested in the quantity of interest in a specific region while the whole domain is our interest in global UQ. Reliability analysis, which quantifies the probability that a quantity of interest is larger than a certain threshold, belongs to local UQ. Analyzing the statistical properties, such as mean, standard deviation, and other moments, falls into global UQ. Both local UQ and global UQ can be performed using brute force MCS. However, MCS is computationally expensive for most computer simulation models. In order to make the UQ of computer simulation models possible, a surrogate model is widely used in UQ to substitute the original simulation model. The widely used surrogate models in UQ studies include Gaussian process model (Kriging model) [102], polynomial chaos expansion (PCE) [15], support vector machine (SVM) [103], and neural networks. Here, we briefly introduce the Kriging model and PCE.

(a) Kriging surrogate modeling

A Kriging model approximates the response of a simulation model by assuming the approximated response as a Gaussian stochastic process [104, 105]. The Kriging model of a simulation model $g(\mathbf{d})$ is given by [104]

$$g(\mathbf{d}) = \mathbf{h}(\mathbf{d})^T\mathbf{v} + \varepsilon(\mathbf{d}) \tag{5}$$

where $\mathbf{d}$ is the vector of input variables, $\mathbf{v} = [v_1,\ v_2,\ \cdots,\ v_p]^T$ is a vector of unknown coefficients, $\mathbf{h}(\mathbf{d}) = [h_1(\mathbf{d}),\ h_2(\mathbf{d}),\ \cdots,\ h_p(\mathbf{d})]^T$ is a vector of regression functions, $\mathbf{h}(\mathbf{d})^T\mathbf{v}$ is the trend of prediction, and $\varepsilon(\mathbf{d})$ is usually assumed to be a Gaussian process with zero mean and covariance $Cov(\varepsilon(\mathbf{d}_i),\ \varepsilon(\mathbf{d}_j))$ given by

$$Cov\left(\varepsilon(\mathbf{d}_i),\ \varepsilon\left(\mathbf{d}_j\right)\right) = \sigma_\varepsilon^2 R\left(\mathbf{d}_i,\ \mathbf{d}_j\right) \tag{6}$$

in which σ_ε^2 is the process variance and $R(\mathbf{d}_i,\ \mathbf{d}_j)$ is the correlation function.

For a new point $\mathbf{d}$, the prediction of the Kriging model follows a Gaussian distribution with the mean and variance of the prediction given by

$$g(\mathbf{d}) = \mathbf{h}(\mathbf{d})^T\mathbf{v} + \mathbf{r}(\mathbf{d})^T\mathbf{R}^{-1}(\mathbf{g}-\mathbf{H}\mathbf{v}) \tag{7}$$

$$\mathrm{MSE}(\mathbf{d}) = \sigma_\varepsilon^2\left\{1-\mathbf{r}(\mathbf{d})^T\mathbf{R}^{-1}\mathbf{r}(\mathbf{d}) + \left[\mathbf{H}^T\mathbf{R}^{-1}\mathbf{r}(\mathbf{d})-\mathbf{h}(\mathbf{d})\right]^T\left(\mathbf{H}^T\mathbf{R}^{-1}\mathbf{H}\right)^{-1}\left[\mathbf{H}^T\mathbf{R}^{-1}\mathbf{r}(\mathbf{d})-\mathbf{h}(\mathbf{d})\right]\right\} \tag{8}$$

where $\mathbf{r}(\mathbf{d}) = [R(\mathbf{d},\ \mathbf{d}_1),\ R(\mathbf{d},\ \mathbf{d}_2),\ \cdots,\ R(\mathbf{d},\ \mathbf{d}_{n_s})]$, $\mathbf{d}_i$ is the ith training point, n_s is the number of training points, $\mathbf{R}$ is the correlation function evaluated at the training points, and $\mathbf{H}$ is the regression function $\mathbf{h}(\mathbf{d})$ evaluated at the training points.

The hyper-parameters of the Kriging model, which include unknown coefficients υ, σ_ε^2, and parameters of $R(\mathbf{d}_i,\ \mathbf{d}_j)$ can be estimated using either maximum likelihood or least squares. More details about Kriging method can be found in [104, 105], and a Kriging toolbox is available in both Python and MATLAB [106].

(b) Polynomial chaos expansion (PCE)

The PCE surrogate modeling method uses a polynomial orthogonal basis to approximate a simulation model. The PCE surrogate model is given by [15]

$$g(\xi) = \sum_{j=0}^{n_b}\omega_j\Psi_j(\xi) \tag{9}$$

where $\Psi_j(\xi)$ is the ith orthogonal basis function, ω_j is the coefficient of the ith orthogonal basis function, and ω_j is the number of basis functions used. For different random

variables, different basis functions should be used. The orthogonal basis functions have the following property

$$\int \Psi_j(\xi)\Psi_k(\xi)\rho(\xi)d\xi = \delta_{j,k} \tag{10}$$

where $\delta_{j,k}$ is Kronecker delta, and $\rho(\xi)$ is PDF of random variables.

The coefficients of the PCE model are solved using the following equation [15]

$$\omega_k = \frac{\langle g,\ \Psi_k\rangle}{\langle \Psi_k,\ \Psi_k\rangle} = \frac{1}{\int \Psi_k^2(\xi)\rho(\xi)d\xi}\int g(\xi)\Psi_k(\xi)\rho(\xi)d\xi \tag{11}$$

The above equation shows that the solving the coefficients ω_k and $k = 1,\ 2,\ \cdots,\ n_b$ is basically solving the integration given in Eq. (11). Since the simulation model $g(\xi)$ is involved in the integration, tensor grid and sparse grid approaches have been investigated to solve the integration [107]. Equation (11) has also been formulated into an optimization problem to minimize the overall regression error by estimating the coefficients using compressive sensing or least square methods [108]. Due to the orthogonal properties of the basis functions, the mean and standard deviation of the response variable can be estimated analytically.

The Kriging surrogate modeling method has also been integrated with PCE method to develop a PCE-Kriging surrogate modeling method in recent years. Advanced Kriging surrogate modeling methods have also been proposed to effectively perform local UQ [16, 109].

There are several research issues that are worth pursuing in the UQ of single model in the AM models. First, there are many sources of uncertainty in the AM process, even for a single simulation model such as the melting pool model. How to effectively reduce the number of training points required for the surrogate modeling given numerous sources of uncertainty is a challenge. Second, there are usually inevitable noises in the simulation models and experiments, such as the powder bed simulation model. Given the noises in the results of simulations and experiments, how to effectively perform UQ of a single model is a challenging issue.

The first challenge can be resolved by resorting to statistical-based surrogate modeling method and taking advantage of currently high-performance computing and big data techniques. The second challenge can be addressed by using Bayesian Gaussian process model or Bayesian PCE model. The noises in the response can be accounted for through the uncertainty in the parameters of the surrogate models. Based on the UQ of single models, we discuss how to effectively perform UQ of the whole AM process.

4.2.2 Multi-level UQ and uncertainty aggregation

As shown in Fig. 2, the modeling of the entire AM process is a multi-level problem. The outputs of lower level models (powder bed model, heat source model) are inputs to the upper level models (i.e., melting pool model and solidification model). In order to propagate uncertainty from process parameters and other environmental parameters to the QoIs at the top level, multi-level UQ methods are required.

As a flexible tool for the multivariate joint probability density modeling, Bayesian networks (BNs) play a vital role in the multi-level UQ of AM process. BNs express the joint probability density of n random variables $X_1,\ X_2,\ \cdots,X_n$ in terms of conditional probabilities as [94]

$$P(\mathbf{X}) = P(X_1,\ X_2,\ \cdots,X_n) = \prod_{i=1}^{n} P(X_i|\pi_i) \tag{12}$$

where π_i is the set of parents nodes of node X_2, and $P(X_i|\pi_i)$ is the conditional probability density function of node X_2 for given realization of its parents. The nodes without parent nodes are called root nodes, such as the process parameters including scan speed, hatch spacing, and others. The probability density functions of the root nodes are obtained from the uncertainty sources modeling discussed in Sect. 4.1.2.

In the multi-level UQ of AM process, each individual simulation model can also be a BN embedded in overall network of the AM process. The surrogate models as discussed in Sect. 4.2.1 can also be subnetworks in the overall BN. The benefits of using BN for the UQ in AM process are multi-fold, as listed below.

- BN can effectively connect various simulation models and mathematical models to facilitate the UQ of the entire AM process.
- BN can also connect simulation models with models established from experiments and expert opinion to perform the UQ.
- Heterogeneous sources of information can be aggregated through BNs to quantify the uncertainty in the quantity of interest.
- BN can also facilitate UM in the AM process to improve the product quality of AM process. Use of BN for UM will be discussed in Sect. 4.3.

Based on the models summarized in Table 1, we provide a schematic network in Fig. 5 to illustrate how various models and parameters can be connected through a BN. Note that a model cannot be node of a BN. Each model in the network is also a BN connecting the input variables and output variables of the model.

In the above network, various parameters and outputs of models are connected with each other through conditional probability density (CPD) functions. In addition to multi-level UQ, there may also be coupling between different simulation models in some of the analysis models (e.g., coupling between finite element model and the cellular automaton model). To address the challenge introduced by the coupling

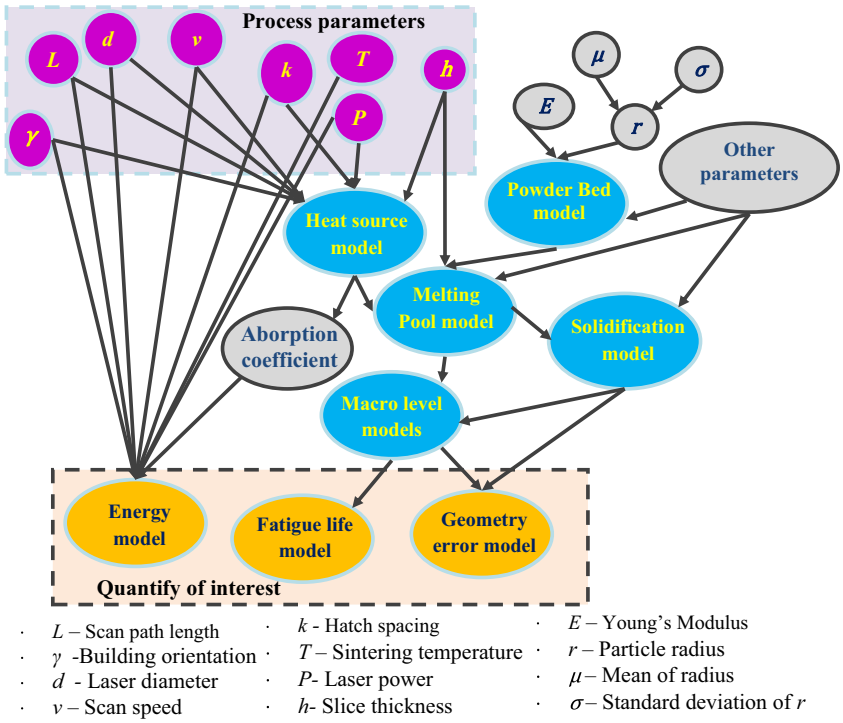

Fig. 5 A schematic network for uncertainty aggregation in the AM process

between different simulation models, decoupling strategies can be employed, such as the first-order reliability method based method and the likelihood-based approach for multi-disciplinary analysis (LAMDA) [110]. Next, we will discuss the model verification and validation based on the uncertainty aggregation.

4.2.3 Model V&V

Model verification and validation (V&V) is the process of determining the agreement to which a model is an accurate representation of the real world from the perspective of the intended use of the model [111, 112]. Before applying the multi-level modeling of the AM process to the design optimization of AM process and UM, the models need to be verified and validated to ensure that the models can be used to represent the actual physics. Model validation can be performed qualitatively or quantitatively. Qualitative validation methods (i.e., graphical comparison) describe the agreement visually, while quantitative methods (using a validation metric) numerically characterize the degree of agreement [113]. Commonly studied quantitative validation metrics include mean-based methods [114, 115], hypothesis testing-based methods [113], area metric [116], and distance or reliability metric [112, 117]. A detailed review of different validation metrics can be found in Ref. [112]. The uncertainty quantified in this section can be effectively incorporated in the validation process using the aforementioned validation metrics.

In the following section, we will discuss how to manage the uncertainty sources in the AM.

4.3 Uncertainty management

This section investigates the UM in AM to answer the following three questions: (1) How to reduce the number of variables in UQ analysis? (2) How to reduce the uncertainty prediction of AM models? (3) How to optimize the process parameters to reduce the effects of uncertainty sources on the AM product quality?

4.3.1 Dimension reduction of random variables

Dimension reduction of the random variables aims to reduce the number of variables considered in the UQ and UM of AM process since not all of the variables are important. An effective method for dimension reduction is global sensitivity analysis (GSA), which ranks the contribution of each input variable (X) on the variance $Var(Y)$ of an output quantity of interest (Y). Sobol' indices are commonly used in this context, which quantify the uncertainty contribution using two kinds of indices: first-order indices and total indices. The first-order index measures the contribution of an individual variable without considering its interactions with other variables and is given by [118]

$$S_i^I = \frac{Var_{X_i}(E_{X_{\sim i}}(Y|X_i))}{Var(Y)} \tag{13}$$

where X_i is the ith input variable, $X_{\sim i}$ is the vector of variables excluding variable X_i, $Var(Y)$ is the variance of quantity of interest (Y), and $E_{X_{\sim i}}(Y|X_i)$ is the expectation by freezing X_i.

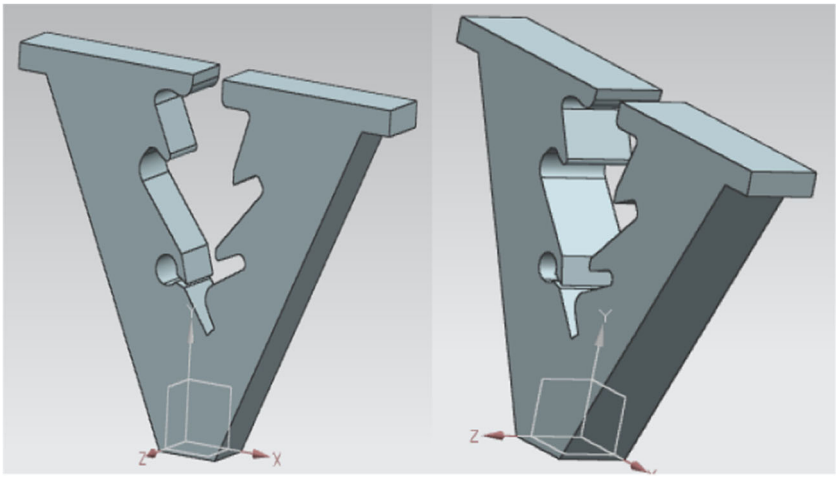

Fig. 6 A 3D model with different building orientations

The total index measures the contribution of an individual variable and its interactions with other variables. The total effect index is given by

$$S_i^T = 1 - \frac{E_{X_{\sim i}}(Var_{X_i}(Y|X_{\sim i}))}{Var(Y)} \quad (14)$$

Based on the results of GSA, the less important random variables can be fixed at certain specific values (usually nominal or mean values) without considering their variability. GSA can be performed both locally and globally. *Locally*, GSA can be performed for individual node of the network as given in Fig. 5. Note that a node of the BN can be the output of a simulation model, a mathematical model, or a surrogate model. When the output of a surrogate model is used, analytical expressions have been derived for the first-order Sobol' indices based on Kriging surrogate model [119] and polynomial chaos expansion [120] methods. *Globally*, the GSA can be performed directly on the BN from the final quantity of interest point of view. To achieve the purpose of GSA on BN, sampling-based method has been recently developed [121].

4.3.2 Resource allocation for uncertainty reduction

As discussed in Sect. 4.1, there are two types of uncertainty in the AM process. The aleatory uncertainty is irreducible while epistemic uncertainty is reducible. For different types of epistemic uncertainty, the methods of uncertainty reduction are different. For instance, the epistemic uncertainty in the parameters of a random variable can be reduced by collecting more experiment data; and the epistemic uncertainty in surrogate model can be reduced by performing more computer simulations (i.e., adding more training points).

In reality, we are usually limited by the available resources (computational and experimental). Given the limited resources, how to effectively reduce the epistemic uncertainty is an important ongoing research issue. It is also an important topic for the uncertainty reduction in the modeling of AM. To achieve this purpose, the following research directions need be pursued.

- *Experimental design for model calibration*: Bayesian calibration represents the epistemic uncertainty in parameters and variables based on prior information and observation data collected from experiments. To maximize the information gain (reduction in the epistemic uncertainty), the experiment input settings need to be optimized [122–124].
- *Adaptive surrogate modeling*: Computer simulation models are usually computationally expensive. To reduce the epistemic uncertainty (bias and variance) introduced by the surrogate model, we need to adaptively determine the optimal input settings for computer simulations and thus maximize the information we obtained from the simulation model for training the surrogate model [16, 109].
- *Resource allocation for experiments and surrogate modeling*: Since both experiments and simulation models are expensive, given the limited computational and experimental resources, how to maximize the reduction of epistemic uncertainty and thus increase the quality of AM process model prediction is a research topic that needs to be investigated [125, 126].
- *Experimental design for model validation*: As discussed in Sect. 4.2.3, model validation needs to be performed to validate the credibility of the models. During the process of model validation, validation experiments need to be performed to collect data for validation. However, not all the data are useful for model validation. How to effectively collect data for validation and thus accelerate the product certification process is an important issue that needs to be addressed. In this regard, the validation experiment design methods developed in Ref. [127] can be explored to perform validation experiment design for AM models.
- *Resource allocation based on integration of model calibration, validation, and UQ*: In the UQ of AM process,

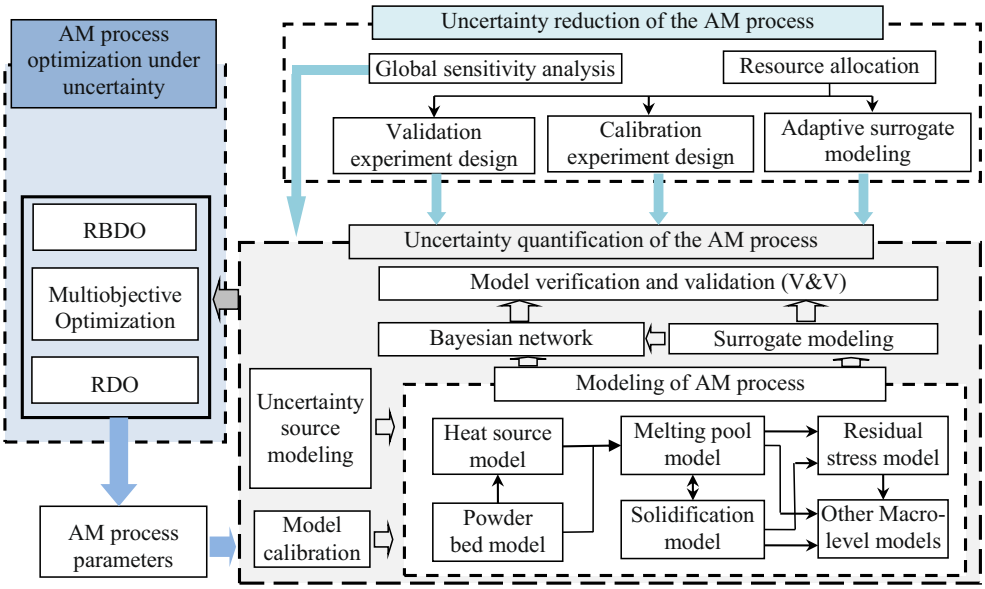

Fig. 7 Overall UQ and UM frameworks of the AM process

model calibration, validation, and forward uncertainty prediction are needed. Different techniques have different motivations. Integration of the results of calibration, validation, and uncertainty prediction can enhance our confidence in the UQ of AM process. To achieve the purpose of integration of calibration, validation, and uncertainty prediction, a roll-up method [128] has been recently developed. Resource allocation based on integration of model calibration, validation, and UQ can reduce the uncertainty in AM models in a symmetric way.

4.3.3 AM process optimization under uncertainty

Since the aleatory uncertainty is irreducible, the process parameters need to be optimized to reduce the effects of aleatory uncertainty on the variability of quantity of interest. As shown in Fig. 6, the optimal building orientation and slice thickness need to be determined to minimize the manufacturing error and standard deviation of the geometry error. The AM process optimization under uncertainty can be pursued in two directions: reliability-based design optimization (RBDO) [129] and robust design optimization (RDO) [130].

In RBDO, the process parameters are optimized while the optimization is subjected to reliability constraints regarding the QoIs. In RDO, the process parameters are optimized such that the QoIs are not sensitive to the variations in the manufacturing environment. During the optimization process, the UQ framework developed in Sect. 4.2 is used to estimate the variations in the QoIs with process parameters as the input variables.

In addition to the conventional RBDO and RDO, advanced RBDO and RDO methods also need to be developed considering that the epistemic uncertainty cannot be completely eliminated and multiple QoIs need to be considered during the optimization process. Such advanced RBDO and RDO methods need to consider both aleatory and epistemic uncertainty [131] and multiple optimization objectives [132, 133].

In the next section, we will summarize the proposed UQ and UM framework for quality control of the AM process.

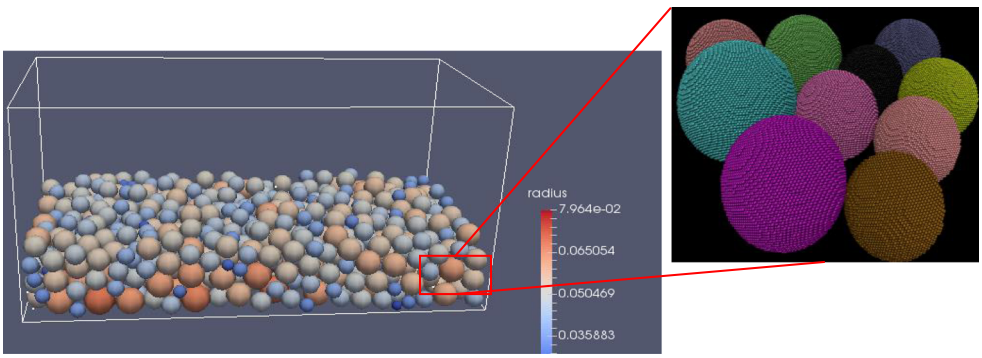

Fig. 8 Illustration of powder bed simulation

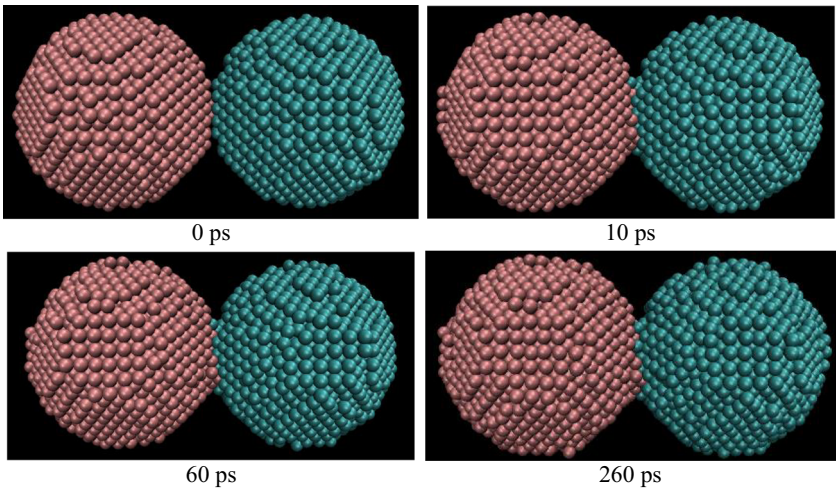

Fig. 9 Laser sintering of two Fe nanoparticles (at different simulation time given in picoseconds)

4.4 Summary of UQ and UM framework

Figure 7 summarizes the proposed overall UQ and UM framework of the AM process as discussed in Sects. 4.1, 4.2, and 4.3. There are mainly four modules: modeling of the AM process, UQ of the AM process based on the process modeling, uncertainty reduction module, and module for AM process optimization under uncertainty. Connections between modules of the overall framework and models in each individual module are also presented in the figure. For example, the AM process optimization under uncertainty module is coupled with the UQ module because UQ needs to be performed under different input settings of the process parameters; the uncertainty reduction module will act as inputs to the UQ module since the collected data from experiment design will be used in the UQ process and affect the result of the UQ process.

In the proposed UQ and UM framework of AM process, some of the research topics have already been intensively studied, such as model calibration and validation. Some of the other research topics need to be further investigated in future research, such as experiment design for model calibration and validation, and optimization under uncertainty of the AM process. Next, we will use an example to illustrate the implementation of some of the techniques presented in the above framework.

5 Example: UQ of the selective laser sintering of nanoparticles

In this section, laser sintering of nanoparticles, which is one of the main steps of the micro-AM process, is used to illustrate the application of the UQ techniques in the AM process. As discussed in Sect. 3, powder bed simulation can be performed first. Figure 8 gives an illustrative example of the powder bed simulation. From the powder bed simulation, we can obtain the radius distribution of the particles as well as the porosity of the powder bed. This information can then be used as inputs for the UQ of melting and solidification models.

In this paper, for the sake of illustration, we use a simplified laser sintering model to investigate the effects of uncertainty sources on the quantity of interest (ultimate tensile strength) of the structure obtained from laser sintering. In the simplified example, two spherical Fe-Fe nanoparticles are first melted under constant heating rate and cooled down under a constant cooling rate. After that, tensile test is performed on the structure to investigate the material properties due to melting and cooling. Simulations of the laser sintering and tensile test of nanoparticles are performed using Large-scale Atomic/Molecular Massively Parallel Simulator (LAMMPS) code [134]. Figures 9 and 10 depict the simulations of the laser sintering and tensile test of the nanoparticles, respectively.

To quantify the uncertainty in the simulation result, we first identify the uncertainty sources. The aleatory uncertainty sources include the variability of particle radii, the uncertainty in the sintering temperature, and the gap between the particles due to packing of powder bed. Since the LAMMPS model is used to simulate the process of sintering and tensile test, the epistemic uncertainty mainly comes from the simulation model. In the LAMMPS simulation, the embedded atom model

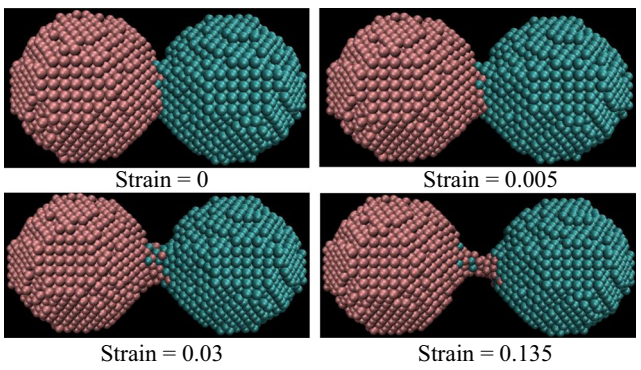

Fig. 10 Tensile test of the nanoparticles obtained from laser sintering

Table 2 Random variables of the laser sintering of nanoparticles

Variable	R_1 (Å)	R_2 (Å)	d (Å)	T (K)	ζ_1	ζ_2	ζ_3	ω_1
Distribution	Gaussian	Gaussian	Gaussian	Gaussian	Gaussian	Gaussian	Gaussian	Gaussian
Mean	22.25	21.75	0.05	1075	11.675	−0.0115	0.475	-3.5×10^{-4}
Standard deviation	0.005	0.005	0.01	15	0.02	5×10^{-3}	0.02	1.75×10^{-5}

(EAM) potential given as below is used to approximate the total energy of an atom [135].

$$E = \sum_{i=1}^{N-1} \sum_{j=i+1}^{N} \varphi(r_{ij}) + \sum_{i=1}^{N} \Phi(\rho_i) \tag{15}$$

where N is the number of atoms in the system, r_{ij} is the distance between atom i and j, and

$$\rho_i = \sum_j \psi(r_{ij}) \tag{16}$$

$$\varphi(r) = \sum_{k=1}^{n^{\varphi}} a_k^{\varphi} \varphi_k(r) \tag{17}$$

$$\Phi(\rho) = \sum_{k=1}^{n^{\Phi}} a_k^{\Phi} \Phi_k(\rho) \tag{18}$$

in which

$$\psi(r) = \sum_{k=1}^{n^{\psi}} \psi_k(r) \tag{19}$$

Ackland et al. [136] and Biersack and Ziegler [137] have fitted the density function and embedded energy function of Fe-Fe potential as follows

$$\psi(r) = \sum_{k=1}^{3} \zeta_k \left(r_k^{\psi} - r\right)^3 \theta\left(r_k^{\psi} - r\right) \tag{20}$$

$$\Phi(\rho) = -\rho^{1/2} + \omega_1 \rho^2 \tag{21}$$

where $r_1^{\psi} = 2.4$, $r_2^{\psi} = 3.2$, $r_3^{\psi} = 4.2$, and $\theta(x)$ are the Heaviside step functions.

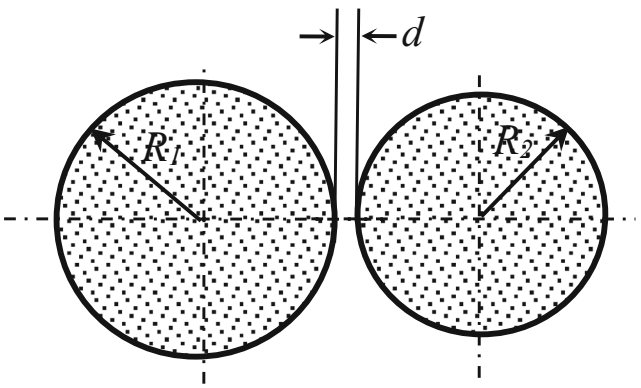

Fig. 11 Illustration of power bed simulation

Since EAM is a regression model based on experiment data, there is uncertainty in the coefficients (ζ_1, ζ_2, ζ_3, and ω_1) of the EAM potentials due to uncertainty in the experiment and limited experiment data. The uncertainty in the coefficients of EAM potentials is epistemic and can be quantified using Bayesian calibration (i.e., Sect. 4.1.2) based on the experiment data. Along with the epistemic uncertainty in the EAM potential coefficients, there is also uncertainty in the LAMMPS simulation result due to the simplification and assumptions made in the molecular dynamics simulations. In this example, the aleatory uncertainty in the geometry and sintering temperature and the epistemic uncertainty in the EAM potential is considered. Table 2 gives the assumed random variables in this example. Variables ζ_1, ζ_2, ζ_3, and ω_1 represent the epistemic uncertainty in the EAM potential, T is the sintering temperature, d is the gap between two nanoparticles, and R_1 and R_2 are the radii of the two nanoparticles. In this example, the distributions are assumed to be Gaussian for the sake of illustration. The method presented in this example is applicable to any kind of distributions. The distributions of the gap between nanoparticles and radii of nanoparticles can be obtained from the powder bed simulation as illustrated in Fig. 8. Figure 11 shows the geometry of two nanoparticles.

Figure 12 plots the strain-stress curve obtained from the tensile test model under a given realization of the random

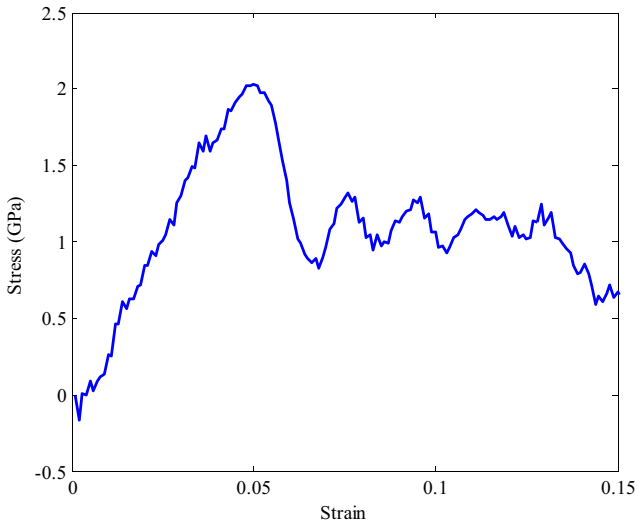

Fig. 12 $R_1 = 22.41$ nm, $R_2 = 21.68$ nm, $T = 1052.6$ K, $d = 0.013$ nm, $\zeta_1 = 11.5961$, $\zeta_2 = -0.0081$, $\zeta_3 = 0.4836$, $\omega_1 = -3.84 \times 10^{-4}$

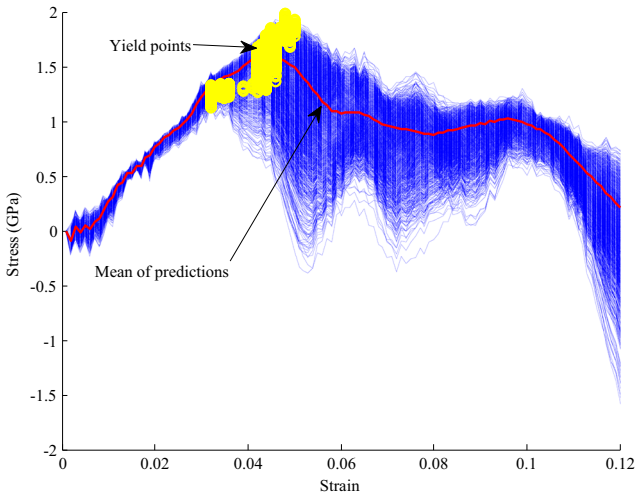

Fig. 13 UQ of the strain-stress curve

variables. Based on the LAMMPS simulation runs, surrogate models are built for the stress response using the Kriging surrogate model method as discussed in Sect. 4.2.1. Based on the surrogate modeling of the laser sintering model, we then perform MCS on the surrogate model to investigate the uncertainty in the strain-stress curve due to the aforementioned uncertainty sources. Figure 13 gives 1000 realizations of the strain-stress curves obtained from MCS. From the samples of the strain-stress curve, we also obtained samples of the ultimate tensile strength of the structure after laser sintering. Figure 14 plots the histogram of the ultimate tensile strength of the structure. The distribution of the ultimate tensile strength can be used in the macro-level model to perform structural reliability analysis.

To analyze the contributions of various sources of uncertainty on the variability of the ultimate tensile strength of the structure, we also performed GSA for the ultimate tensile strength using the method presented in Sect. 4.3.1. Figure 15

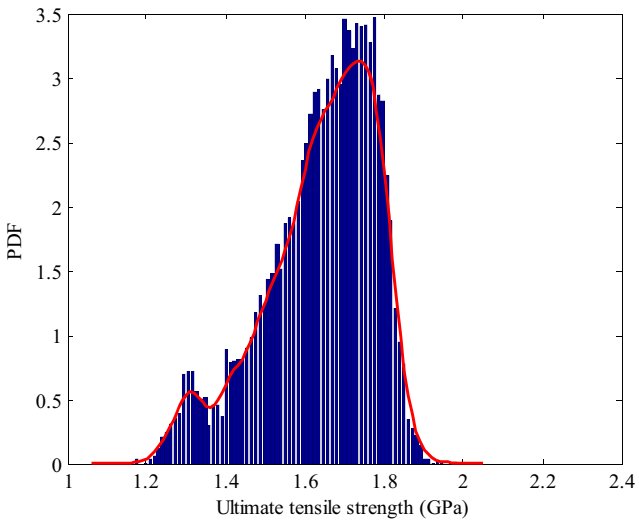

Fig. 14 Distribution of the ultimate tensile strength

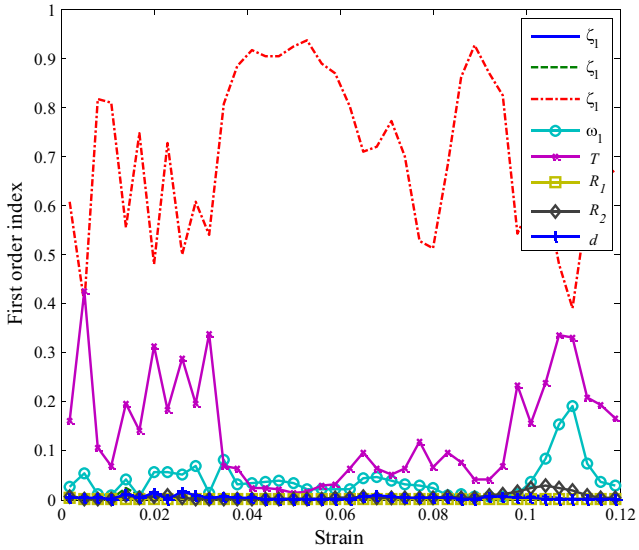

Fig. 15 GSA of the ultimate tensile strength

gives the first-order Sobol' indices obtained from GSA under different strain values. The results show that the epistemic uncertainty in the EAM potential makes the most significant contribution to the uncertainty in the ultimate tensile strength for the studied case. Next, the sintering temperature also makes major a contribution to the uncertainty of tensile strength. In this example, the contributions of radii of nanoparticles and gap between nanoparticles are very small. One possible reason is that the standard deviations of the radii and gap as given in Table 2 are very small.

In this example, we illustrated the application of surrogate modeling, MCS, and GSA in the laser sintering (melting and cooling) of the micro-AM process. Similar procedure can be applied to other individual models as well in the AM process.

6 Summary

AM has shown significant market potential in the production of metal components with complicated geometries. The variation in the quality of products manufactured from AM process, however, has impeded the wide application of the AM technology. To resolve this issue, a better understanding of the causes of the variation in the quality of products is required. This paper discusses the needs and opportunities in the UQ and UM of AM process. Research needs and directions of UQ and UM in AM process are studied based on the review of currently available AM process models. A UQ and UM framework is proposed for the AM process to reduce the effects of uncertainty sources on the AM product quality. An example of laser sintering of nanoparticle is used to illustrate the implementation procedure of several techniques in the proposed UQ and UM framework.

Future needs include investigating new UQ and UM techniques to meet the requirement of the AM process, developing multi-scale and multi-physics models for the AM process, and applying UQ and UM techniques to the AM process.

Acknowledgements The research reported in this paper was supported by funds from the National Institute of Standards and Technology under the Smart Manufacturing Data Analytics Project (Cooperative Agreement No. 70NANB14H036) and Air Force Office of Scientific Research (Grant No. FA9550-15-1-0018, Technical Monitor: Dr. David Stargel). The support is gratefully acknowledged. The authors would also like to thank Mr. Shou Wan at Missouri University of Science and Technology for helping with the sintering simulation.

References

1. Standard A (2012) F2792. 2012. Standard terminology for additive manufacturing technologies, ASTM F2792-10e1
2. Huang Y, Leu MC, Mazumder J, Donmez A (2015) Additive manufacturing: current state, future potential, gaps and needs, and recommendations. J Manuf Sci Eng 137(1):014001
3. Vaezi M, Seitz H, Yang S (2013) A review on 3D micro-additive manufacturing technologies. Int J Adv Manuf Technol 67(5–8): 1721–1754
4. Wohler T (2013) "Additive manufacturing and 3D printing—state of the industry annual worldwide progress report 2014, Wohler's associates," Inc., Fort Collins, CO
5. Zhang X, Jiang X, Sun C (1999) Micro-stereolithography of polymeric and ceramic microstructures. Sensors Actuators A Phys 77(2):149–156
6. Mireles J, Kim H-C, Lee IH, Espalin D, Medina F, MacDonald E, Wicker R (2013) Development of a fused deposition modeling system for low melting temperature metal alloys. J Electron Packag 135(1):011008
7. Klosterman D, Chartoff R, Graves G, Osborne N, Priore B (1998) Interfacial characteristics of composites fabricated by laminated object manufacturing. Compos A: Appl Sci Manuf 29(9):1165–1174
8. Lü L, Fuh JYH, Wong Y-S (2001) "Selective laser sintering," Laser-Induced Materials and Processes for Rapid Prototyping, Springer, pp. 89–142
9. Kruth J-P, Froyen L, Van Vaerenbergh J, Mercelis P, Rombouts M, Lauwers B (2004) Selective laser melting of iron-based powder. J Mater Process Technol 149(1):616–622
10. Dinda G, Dasgupta A, Mazumder J (2009) Laser aided direct metal deposition of Inconel 625 superalloy: microstructural evolution and thermal stability. Mater Sci Eng A 509(1):98–104
11. Tang L, Ruan J, Landers RG, Liou F (2008) Variable powder flow rate control in laser metal deposition processes. J Manuf Sci Eng 130(4):041016
12. Morgan R, Sutcliffe C, O'neill W (2004) Density analysis of direct metal laser re-melted 316L stainless steel cubic primitives. J Mater Sci 39(4):1195–1205
13. Tapia G, Elwany A (2014) A review on process monitoring and control in metal-based additive manufacturing. J Manuf Sci Eng 136(6):060801
14. Hu Z, Mahadevan S, Du X "Uncertainty quantification in time-dependent reliability analysis in the presence of parametric uncertainty," ASCE-ASME J Risk Uncertain Eng Syst, B: Mech Eng
15. Xiu D, Karniadakis GE (2002) The Wiener–Askey polynomial chaos for stochastic differential equations. SIAM J Sci Comput 24(2):619–644
16. Bichon BJ, Eldred MS, Swiler LP, Mahadevan S, McFarland JM (2008) Efficient global reliability analysis for nonlinear implicit performance functions. AIAA J 46(10):2459–2468
17. Kamath C, (2016) "Data mining and statistical inference in selective laser melting," The International Journal of Advanced Manufacturing Technology, pp. 1-19.
18. Lopez F, Witherell P, Lane B (2016) Identifying uncertainty in laser powder bed fusion additive manufacturing models. Journal of Mechanical Design 138(11):114502
19. Moser D, Beaman J, Fish S, Murthy J (2014) "Multi-layer computational modeling of selective laser sintering processes." ASME 2014 International Mechanical Engineering Congress and Exposition, Volume 2A: Advanced Manufacturing. Montreal, Quebec, Canada, November 14–20, Paper No. IMECE2014-37535, pp. V02AT02A008; 11 pages
20. Turner JA, Babu SS, Blue C (2015) "Advanced Simulation for Additive Manufacturing: Meeting Challenges Through Collaboration (Workshop Report for U.S. DOE/EERE/AMO),", Oak Ridge National Laboratory, ORNL Report TM-2015/324, Sep, 2015
21. Mellor S, Hao L, Zhang D (2014) Additive manufacturing: a framework for implementation. Int J Prod Econ 149:194–201
22. Baumers M, Tuck C, Bourell D, Sreenivasan R, Hague R (2011) "Sustainability of additive manufacturing: measuring the energy consumption of the laser sintering process," Proceedings of the Institution of Mechanical Engineers. Part B: Journal of Engineering Manufacture 225(12):2228–2239
23. Paul R, Anand S (2012) Process energy analysis and optimization in selective laser sintering. J Manuf Syst 31(4):429–437
24. Nelson JC, Xue S, Barlow JW, Beaman JJ, Marcus HL, Bourell DL (1993) Model of the selective laser sintering of bisphenol-A polycarbonate. Ind Eng Chem Res 32(10):2305–2317
25. Zäh MF, Lutzmann S (2010) Modelling and simulation of electron beam melting. Prod Eng 4(1):15–23
26. Rubenchik A, Wu S, Mitchell S, Golosker I, LeBlanc M, Peterson N (2015) Direct measurements of temperature-dependent laser absorptivity of metal powders. Appl Opt 54(24):7230–7233
27. King W, Anderson A, Ferencz R, Hodge N, Kamath C, Khairallah S, Rubenchik A (2015) Laser powder bed fusion additive manufacturing of metals; physics, computational, and materials challenges. Appl Phys Rev 2(4):041304
28. Markl M, Körner C (2016) Multi-scale modeling of powder-bed-based additive manufacturing. Annu Rev Mater Res 46:1–34
29. Wang X, Kruth J (2000) "Energy absorption and penetration in selective laser sintering: a ray tracing model.", In Proceedings of the International Conference on Mathematical Modeling and Computer Simulation of Metal Technologies, Ariel, Israel, November 13-15, MMT (pp. 673-682)
30. Boley C, Khairallah S, Rubenchik A (2015) Calculation of laser absorption by metal powders in additive manufacturing. Appl Opt 54(9):2477–2482
31. Meakin P, Jullien R (1987) Restructuring effects in the rain model for random deposition. J Phys 48(10):1651–1662
32. Mishra B, Rajamani RK (1992) The discrete element method for the simulation of ball mills. Appl Math Model 16(11):598–604
33. Kloss C, Goniva C (2011) LIGGGHTS—open source discrete element simulations of granular materials based on Lammps. Supplemental Proceedings: Materials Fabrication, Properties, Characterization, and Modeling 2:781–788
34. Dou X, Mao Y, Zhang Y (2014) Effects of contact force model and size distribution on microsized granular packing. J Manuf Sci Eng 136(2):021003
35. Xiang Z, Yin M, Deng Z, Mei X, Yin G (2016) Simulation of forming process of powder bed for additive manufacturing. J Manuf Sci Eng 138(8):081002

36. Herbold, E., Walton, O., and Homel, M., 2015, "Simulation of powder layer deposition in additive manufacturing processes using the discrete element method," Lawrence Livermore National Lab.(LLNL), Livermore, CA (United States).
37. Parteli EJR. (2013) "DEM simulation of particles of complex shapes using the multisphere method: application for additive manufacturing." In AIP Conference Proceedings, vol. 1542, no. 1, pp. 185-188. AIP, doi: 10.1063/1.4811898
38. Alexander FJ, Chen S, Sterling J (1993) Lattice Boltzmann thermohydrodynamics. Phys Rev E 47(4):R2249
39. Khairallah SA, Anderson A (2014) Mesoscopic simulation model of selective laser melting of stainless steel powder. J Mater Process Technol 214(11):2627–2636
40. Devesse W, De Baere D, Guillaume P (2014) The isotherm migration method in spherical coordinates with a moving heat source. Int J Heat Mass Transf 75:726–735
41. Jasak, H., Jemcov, A., and Tukovic, Z., "OpenFOAM: a C++ library for complex physics simulations," Proc. International Workshop on Coupled Methods in Numerical Dynamics, IUC Dubrovnik, Croatia, pp. 1–20.
42. Klassen A, Scharowsky T, Körner C (2014) Evaporation model for beam based additive manufacturing using free surface lattice Boltzmann methods. J Phys D Appl Phys 47(27):275303
43. Gürtler F-J, Karg M, Leitz K-H, Schmidt M (2013) Simulation of laser beam melting of steel powders using the three-dimensional volume of fluid method. Phys Procedia 41:881–886
44. McClelland MA, Maienschein JL, Nichols AL, Wardell JF, Atwood AI, Curran PO (2002) "ALE3D Model Predictions and Materials Characterization for the Cookoff Response of PBXN-109", (No. UCRL-JC-145756). Lawrence Livermore National Lab., CA (US)
45. Qi Y, Çağın T, Kimura Y, Goddard WA III (1999) Molecular-dynamics simulations of glass formation and crystallization in binary liquid metals: Cu-Ag and Cu-Ni. Phys Rev B 59(5):3527
46. Rappaz M, Gandin C-A (1993) Probabilistic modelling of microstructure formation in solidification processes. Acta Metall Mater 41(2):345–360
47. Zhang J, Liou F, Seufzer W, Taminger K (2016) A coupled finite element cellular automaton model to predict thermal history and grain morphology of Ti-6Al-4V during direct metal deposition (DMD). Additive Manufac 11:32–39
48. Liou, F., Newkirk, J., Fan, Z., Sparks, T., Chen, X., Fletcher, K., Zhang, J., Zhang, Y., Kumar, K. S., and Karnati, S., 2015, Multiscale and multiphysics modeling of additive manufacturing of advanced materials
49. Amine T, Newkirk JW, Liou F (2015) Methodology for studying effect of cooling rate during laser deposition on microstructure. J Mater Eng Perform 24(8):3129–3136
50. Denlinger, E. R., Heigel, J. C., and Michaleris, P., 2014, Residual stress and distortion modeling of electron beam direct manufacturing Ti-6Al-4V. Proceedings of the Institution of Mechanical Engineers, Part B: Journal of Engineering Manufacture, p. 0954405414539494.
51. Mercelis P, Kruth J-P (2006) Residual stresses in selective laser sintering and selective laser melting. Rapid Prototyp J 12(5):254–265
52. Liu H (2014) "Numerical analysis of thermal stress and deformation in multi-layer laser metal deposition process.", Department of Mechanical and Aerospace Engineering, Missouri University of Science and Technology, master's dissertation, Rolla, Missouri
53. Ding D, Pan Z, Cuiuri D, Li H (2015) Wire-feed additive manufacturing of metal components: technologies, developments and future interests. Int J Adv Manuf Technol 81(1–4):465–481
54. Megahed M, Mindt H-W, N'Dri N, Duan H, Desmaison O (2016) Metal additive-manufacturing process and residual stress modeling. Integrat Mater Manuf Innov 5(1):1–33
55. Paul R, Anand S (2015) A combined energy and error optimization method for metal powder based additive manufacturing processes. Rapid Prototyp J 21(3):301–312
56. Xu X, Meteyer S, Perry N, Zhao YF (2015) Energy consumption model of binder-jetting additive manufacturing processes. Int J Prod Res 53(23):7005–7015
57. Meteyer S, Xu X, Perry N, Zhao YF (2014) Energy and material flow analysis of binder-jetting additive manufacturing processes. Procedia CIRP 15:19–25
58. Garg, A., Lam, J. S. L., and Savalani, M., 2015, "Energy component in the density of selective laser melting fabricated prototype," The International Journal of Advanced Manufacturing Technology, pp. 1-9.
59. Paul R (2013) "Modeling and optimization of powder based additive manufacturing (AM) processes.", Department of Mechanical Engineering, University of Cincinnati, Ph.D. Dissertation
60. Sreenivasan R, Goel A, Bourell D (2010) Sustainability issues in laser-based additive manufacturing. Phys Procedia 5:81–90
61. Körner C, Attar E, Heinl P (2011) Mesoscopic simulation of selective beam melting processes. J Mater Process Technol 211(6): 978–987
62. Mahale TR (2009) "Electron beam melting of advanced materials and structures.", Department of Industrial Engineering, North Carolina State University, Ph.D. Dissertation
63. Gusarov A, Kruth J-P (2005) Modelling of radiation transfer in metallic powders at laser treatment. Int J Heat Mass Transf 48(16): 3423–3434
64. Gusarov A, Yadroitsev I, Bertrand P, Smurov I (2007) Heat transfer modelling and stability analysis of selective laser melting. Appl Surf Sci 254(4):975–979
65. Wang X, Laoui T, Bonse J, Kruth J-P, Lauwers B, Froyen L (2002) Direct selective laser sintering of hard metal powders: experimental study and simulation. Int J Adv Manuf Technol 19(5):351–357
66. Sisto A, Kamath C (2013)" Ensemble Feature Selection in Scientific Data Analysis", Lawrence Livermore National Laboratory (LLNL), Livermore, CA, report number: No. LLNL-TR-644160
67. Tolochko NK, Khlopkov YV, Mozzharov SE, Ignatiev MB, Laoui T, Titov VI (2000) Absorptance of powder materials suitable for laser sintering. Rapid Prototyp J 6(3):155–161
68. Shi Y, Zhang Y (2008) "Simulation of random packing of spherical particles with different size distributions.", ASME 2006 International Mechanical Engineering Congress and Exposition, Heat Transfer, Volume 3, Chicago, Illinois, USA, November 5 – 10, Paper No. IMECE2006-15271, pp. 539-544; 6 pages
69. Parteli EJ, Pöschel T (2016) Particle-based simulation of powder application in additive manufacturing. Powder Technol 288:96–102
70. N'Dri, N., Mindt, H. W., Shula, B., Megahed, M., Peralta, A., Kantzos, P., and Neumann, J., 2015, "DMLS process modelling & validation," TMS2015 Supplemental Proceedings, pp. 389-396.
71. Körner C, Pohl T, Rüde U, Thürey N, Zeiser T (2006) "Parallel lattice Boltzmann methods for CFD applications.", In Numerical Solution of Partial Differential Equations on Parallel Computers, Lecture Notes in Computational Science and Engineering, vol 51. Springer, Berlin, Heidelberg, pp. 439-466
72. Ammer R, Markl M, Ljungblad U, Körner C, Rüde U (2014) Simulating fast electron beam melting with a parallel thermal free surface lattice Boltzmann method. Comput Math Appl 67(2):318–330
73. Mindt H, Megahed M, Perlata A, Neumann J (2015) "DMLM models-numerical assessment of porosity," proceedings from the 22nd International Symposium on Air Breathing Engines, Phoenix, AZ, Oct, pp. 25-30

74. Jahanshahi M, Sanati M, Babaei Z (2008) Optimization of parameters for the fabrication of gelatin nanoparticles by the Taguchi robust design method. J Appl Stat 35(12):1345–1353
75. Boettinger WJ, Warren JA, Beckermann C, Karma A (2002) Phase-field simulation of solidification. Mater Res 32(1):163
76. Beckermann C, Diepers H-J, Steinbach I, Karma A, Tong X (1999) Modeling melt convection in phase-field simulations of solidification. J Comput Phys 154(2):468–496
77. Dai K, Shaw L (2006) Parametric studies of multi-material laser densification. Mater Sci Eng A 430(1):221–229
78. Zaeh MF, Branner G (2010) Investigations on residual stresses and deformations in selective laser melting. Prod Eng 4(1):35–45
79. Cohen, D. L., 2010, "Additive manufacturing of functional constructs under process uncertainty," Cornell University
80. Delgado J, Ciurana J, Rodríguez CA (2012) Influence of process parameters on part quality and mechanical properties for DMLS and SLM with iron-based materials. Int J Adv Manuf Technol 60(5–8):601–610
81. Raghunath N, Pandey PM (2007) Improving accuracy through shrinkage modelling by using Taguchi method in selective laser sintering. Int J Mach Tools Manuf 47(6):985–995
82. Garg A, Tai K, Savalani M (2014) State-of-the-art in empirical modelling of rapid prototyping processes. Rapid Prototyp J 20(2):164–178
83. Schaaf K (1999) "Uncertainty and sensitivity analysis of the heat transfer mechanisms in the lower head.", Proceedings of the OECD/CSNI Workshop on in-vessel core debris retention and coolability, Garching, 3rd-6th March, Paper No. NEA-CSNI-R–1998-18
84. Swiler, L. P., Eldred, M. S., and Adams, B. M., 2015, Dakota: bridging advanced scalable uncertainty quantification algorithms with production deployment
85. Anderson A (2015) "Development of Physics-Based Numerical Models for Uncertainty Quantification of Selective Laser Melting Processes-2015 Annual Progress Report," Lawrence Livermore National Laboratory (LLNL), Livermore, CA, report number: LLNL-TR-678006
86. Adamczak S, Bochnia J, Kaczmarska B (2014) Estimating the uncertainty of tensile strength measurement for a photocured material produced by additive manufacturing. Metrol Measur Syst 21(3):553–560
87. Ma, L., Fong, J., Lane, B., Moylan, S., Filliben, J., Heckert, A., and Levine, L., "Using design of experiments in finite element modeling to identify critical variables for laser powder bed fusion," Proc. International Solid Freeform Fabrication Symposium, Laboratory for Freeform Fabrication and the University of Texas Austin, TX, USA
88. Loughnane, G. T., 2015, "A framework for uncertainty quantification in microstructural characterization with application to additive manufacturing of Ti-6Al-4V," Wright State University
89. Park S-I, Rosen DW, Choi S-k, Duty CE (2014) Effective mechanical properties of lattice material fabricated by material extrusion additive manufacturing. Additive Manufac 1:12–23
90. Cai G, Mahadevan S (2016)" Uncertainty Quantification of Manufacturing Process Effects on Macro-scale Material Properties". International Journal for Multiscale Computational Engineering, 14(3), DOI: 10.1615/IntJMultCompEng.2016015552
91. Haldar A, Mahadevan S (2000) Probability, reliability, and statistical methods in engineering design. **Wiley**, New York
92. Sankararaman S, Ling Y, Mahadevan S (2011) Uncertainty quantification and model validation of fatigue crack growth prediction. Eng Fract Mech 78(7):1487–1504
93. Devathi, H., Hu, Z., and Mahadevan, S., 2016, "Snap-through buckling reliability analysis under spatiotemporal variability and epistemic uncertainty," AIAA J, pp 3981–3993.
94. Mahadevan S, Zhang R, Smith N (2001) Bayesian networks for system reliability reassessment. Struct Saf 23(3):231–251
95. Zhang R, Mahadevan S (2000) Model uncertainty and Bayesian updating in reliability-based inspection. Struct Saf 22(2):145–160
96. Du X (2008) Unified uncertainty analysis by the first order reliability method. Journal of Mechanical Design 130(9):091401
97. Sankararaman S, Mahadevan S (2011) Likelihood-based representation of epistemic uncertainty due to sparse point data and/or interval data. Reliab Eng Syst Saf 96(7):814–824
98. Hu Z, Du X (2015) A random field approach to reliability analysis with random and interval variables. ASCE-ASME J Risk Uncertain Eng Syst B: Mech Eng 1(4):041005
99. Richardson LF (1911) "The approximate arithmetical solution by finite differences of physical problems involving differential equations, with an application to the stresses in a masonry dam," Philosophical Transactions of the Royal Society of London. Ser A, Contain Papers Math Phys Char 210:307–357
100. Celik I, Karatekin O (1997) Numerical experiments on application of Richardson extrapolation with nonuniform grids. J Fluids Eng 119(3):584–590
101. Kennedy MC, O'Hagan A (2001) Bayesian calibration of computer models. J Royal Stat Soc: Ser B (Stat Methodol) 63(3):425–464
102. Jones DR, Schonlau M, Welch WJ (1998) Efficient global optimization of expensive black-box functions. J Glob Optim 13(4):455–492
103. Suykens JA, Vandewalle J (1999) Least squares support vector machine classifiers. Neural Process Lett 9(3):293–300
104. Rasmussen CE, Williams CK (2006) Gaussian processes for machine learning (Vol. 1). Cambridge: MIT press
105. Santner TJ, Williams BJ, Notz WI (2013) "The design and analysis of computer experiments.", Springer Series in Statistics, Springer Science & Business Media New York, DOI 10.1007/978-1-4757-3799-8
106. Lophaven SN, Nielsen HB, Søndergaard J (2002) "DACE-A Matlab Kriging Toolbox, Version 2.0," Technical University of Denmark, Technical. Report No. IMM-TR-2002-12
107. Ganapathysubramanian B, Zabaras N (2007) Sparse grid collocation schemes for stochastic natural convection problems. J Comput Phys 225(1):652–685
108. Hampton J, Doostan A (2015) Compressive sampling of polynomial chaos expansions: convergence analysis and sampling strategies. J Comput Phys 280:363–386
109. Hu Z, Mahadevan S (2016) Global sensitivity analysis-enhanced surrogate (GSAS) modeling for reliability analysis. Struct Multidiscip Optim 53(3):501–521
110. Sankararaman S, Mahadevan S (2012) Likelihood-based approach to multidisciplinary analysis under uncertainty. J Mech Des 134(3):031008
111. Committee, A. S., 1998, "AIAA guide for the verification and validation of computational fluid dynamics simulations (G-077-1998)," AIAA
112. Ling Y, Mahadevan S (2013) Quantitative model validation techniques: new insights. Reliab Eng Syst Saf 111:217–231
113. Rebba R, Mahadevan S, Huang S (2006) Validation and error estimation of computational models. Reliab Eng Syst Saf 91(10):1390–1397
114. Kleijnen JP (1995) Verification and validation of simulation models. Eur J Oper Res 82(1):145–162
115. Drignei D, Mourelatos ZP, Kokkolaras M, Pandey V (2014) Reallocation of testing resources in validating optimal designs using local domains. Struct Multidiscip Optim 50(5):825–838
116. Ferson S, Oberkampf WL, Ginzburg L (2008) Model validation and predictive capability for the thermal challenge problem. Comput Methods Appl Mech Eng 197(29):2408–2430
117. Rebba R, Mahadevan S (2008) Computational methods for model reliability assessment. Reliab Eng Syst Saf 93(8):1197–1207

118. Li C, Mahadevan S (2016) An efficient modularized sample-based method to estimate the first-order Sobol′ index. Reliab Eng Syst Saf 153:110–121
119. Chen W, Jin R, Sudjianto A (2005) Analytical variance-based global sensitivity analysis in simulation-based design under uncertainty. J Mech Des 127(5):875–886
120. Sudret B (2008) Global sensitivity analysis using polynomial chaos expansions. Reliab Eng Syst Saf 93(7):964–979
121. Computers and Information in Engineering Conference. Volume 1A: 36th Computers and Information in Engineering Conference Charlotte, North Carolina, USA, August 21–24, Paper No. DETC2016-59671, pp. V01AT02A023; 10 pages doi:10.1115/DETC2016-59671
122. Hu Z, Ao D, Mahadevan S (2017) Calibration experimental design considering field response and model uncertainty. Computer Methods in Applied Mechanics and Engineering 318:92–119
123. Ao D, Hu Z, Mahadevan S (2017) Design of validation experiments for life prediction models. Reliability Engineering & System Safety 165:22–33
124. Nath P, Hu Z, Mahadevan S (2017) Sensor placement for calibration of spatially varying model parameters. Journal of Computational Physics 343:150–169
125. Sankararaman S, McLemore K, Mahadevan S, Bradford SC, Peterson LD (2013) Test resource allocation in hierarchical systems using Bayesian networks. AIAA J 51(3):537–550
126. Mullins J, Mahadevan S (2014) Variable-fidelity model selection for stochastic simulation. Reliab Eng Syst Saf 131:40–52
127. Jiang X, Mahadevan S (2006) Bayesian cross-entropy methodology for optimal design of validation experiments. Meas Sci Technol 17(7):1895
128. Sankararaman S, Mahadevan S (2015) Integration of model verification, validation, and calibration for uncertainty quantification in engineering systems. Reliab Eng Syst Saf 138:194–209
129. Du X, Chen W (2004) Sequential optimization and reliability assessment method for efficient probabilistic design. J Mech Des 126(2):225–233
130. Zaman K, McDonald M, Mahadevan S, Green L (2011) Robustness-based design optimization under data uncertainty. Struct Multidiscip Optim 44(2):183–197
131. Zaman, K., and Mahadevan, S., 2016, Reliability-based design optimization of multidisciplinary system under aleatory and epistemic uncertainty. Struct Multidiscip Optim, pp. 1-19
132. Rangavajhala S, Mahadevan S (2013) Design optimization for robustness in multiple performance functions. Struct Multidiscip Optim 47(4):523–538
133. Du X, Sudjianto A, Chen W (2004) An integrated framework for optimization under uncertainty using inverse reliability strategy. J Mech Des 126(4):562–570
134. Plimpton, S., Crozier, P., and Thompson, A., 2007, "LAMMPS-large-scale atomic/molecular massively parallel simulator," Sandia National Laboratories, 18
135. Mendelev M, Han S, Srolovitz D, Ackland G, Sun D, Asta M (2003) Development of new interatomic potentials appropriate for crystalline and liquid iron. Philos Mag 83(35):3977–3994
136. Ackland G, Bacon D, Calder A, Harry T (1997) Computer simulation of point defect properties in dilute Fe–Cu alloy using a many-body interatomic potential. Philos Mag A 75(3):713–732
137. Biersack J, Ziegler J (1982) Refined universal potentials in atomic collisions. Nucl Inst Methods Phys Res A 194(1):93–100